Surface Viscoelastic Properties of Spread Films of a Polysilylene−Poly(ethylene oxide) Multiblock Copolymer at the Air−Water Interface

A. J. Milling,[†] R. W. Richards,*[,†] R. C. Hiorns,[‡] and R. G. Jones[‡]

IRC in Polymer Science and Technology, University of Durham, Durham DH1 3LE, UK, and Centre for Materials Research, School of Physical Sciences, University of Kent, Canterbury, Kent CT2 7NR, UK

Received April 27, 1999; Revised Manuscript Received October 26, 1999

ABSTRACT: The viscoelastic properties of a spread layer of a poly(ethylene oxide)-*co*-poly(methylphenylsilylene) alternating block copolymer at the air−water interface have been obtained by surface quasi-elastic light scattering over a range of surface concentrations at a fixed capillary wavenumber and as a function of wavenumber for two surface concentrations. The frequency and the damping for a fixed capillary wavenumber showed a maximum at a surface concentration of 0.8 mg m^{-2}, where resonance between the capillary and dilational waves of the surface film occurs. The surface viscoelastic parameters, i.e., surface tension, dilational modulus, and dilational viscosity, were obtained from the heterodyne correlation functions of the scattered light by direct spectral fitting. The surface tension obtained from light scattering data showed the same qualitative dependence on surface concentration as that from the surface pressure data; however, the light scattering values were somewhat larger, indicating the presence of relaxation processes. Attempts to determine the nature of the relaxation process were made by obtaining the surface viscoelastic parameters as a function of surface wavenumber at the surface concentration where resonance between the surface modes is evident. However, the frequency dependence of the surface moduli followed none of the expectations for simple models of the relaxation process. Close analysis of the capillary wave frequency and damping as a function of surface wavenumber indicated that capillary and dilational modes were *mixed* at the resonance condition. The possibility of a splay mode of aggregated silylene blocks contributing to surface wave dynamics has been discussed.

Introduction

Polysilylenes, otherwise called polysilanes, consist of a linear chain backbone of silicon atoms bearing two substituents that are usually unsubstituted aryl or alkyl groups; see Schemes 1 and 2. They represent a relatively new class of polymeric materials with useful electronic properties.[1] For example, they have been shown to have potential for application as photoresist materials,[2−4] photoconductors,[5,6] and nonlinear optical (NLO) materials.[7−9] In addition, they have found application as photoinitiators in radical polymerization[10,11] and as ceramic precursors.[12,13] Many of the useful properties of polysilylenes can be associated with the delocalization of the σ-electrons of the polymer backbone which manifests as a strong UV absorption, commonly in the wavelength range 300−350 nm.[14,15] However, contrasting with the interesting spectroscopic and electroactive properties, the polymers usually have poor mechanical properties which severely constrain the exploitation of their potential applications. Typically, poly(methylphenylsilylene) is a brittle polymer, a property that can readily be attributed to the polymer chain being comprised predominantly of all-trans sequences such that it is best described as having a wormlike structure in both solution and the solid state. The incorporation of silylene chains within block copolymers might overcome such a detractive feature, and a number have been reported.[16−20] Recently, an amphiphilic multiblock copolymer of poly(methylphenylsilylene), PMPS, and poly(ethylene oxide), PEO, has been shown to form supramolecular structures.[21] Vesicles form in aqueous dispersion while within 75% water/25% tetrahydrofuran, THF, fibers have been characterized. These roll up into helices when the water content of the mixture is increased to 90%.[22] The ease with which the polymer undergoes such self-assembly is attributed to the semirigidity of the PMPS blocks in all-trans sequence. It is this polymer which is the subject of the present study.

Scheme 1

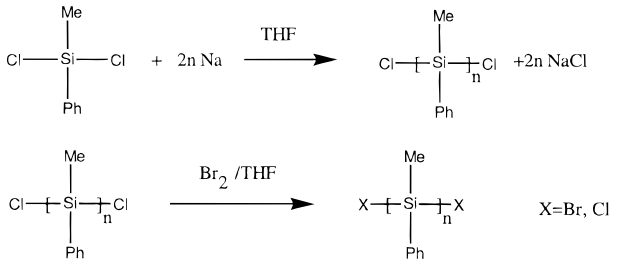

Scheme 2

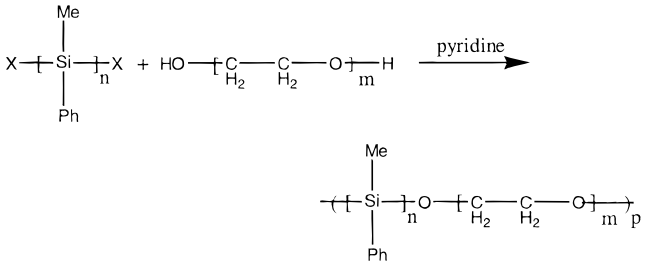

The organization of amphiphilic polymers at the air−water interface has been clarified to some extent by the

[†] University of Durham.
[‡] University of Kent.
* To whom correspondence should be addressed.

10.1021/ma990654w CCC: $19.00
Published on Web 03/16/2000

application of neutron reflectometry to spread films.[23−28] In tandem with these investigations, the role of the spread polymer in modifying the capillary fluctuations of the liquid interface has also been explored.[29−32] The debate over the interpretation of some of the surface dynamic parameters not withstanding,[33] it is evident that the properties of the capillary waves are markedly influenced by the organization of the polymer at the interface. Consequently, there is the possibility of eliciting some information regarding the behavior of polymers at fluid interfaces from a relatively inexpensive technique rather than recourse to neutron reflectivity. The technique used, surface quasi-elastic light scattering (SQELS), has been much applied to pure liquids and surfactant solutions,[34−43] but the application to polymeric films to any significant extent is only a recent development. Nonetheless, SQELS has been responsible for a new theoretical description of polymer modified capillary waves derived from a molecular viewpoint as opposed to the previous phenomenological descriptions.[33]

The range of polymers studied thus far is not large. It is prerequisite that the polymers should spread at the fluid interface, and since the most commonly used liquid is water, the range of suitable polymers is thus restricted. Apart from simple homopolymers, graft and block copolymers have also been investigated by SQELS. Hitherto, the block copolymers used have all been simple linear diblocks. Here we discuss the SQELS investigation of a multiblock copolymer comprised of poly(ethylene oxide) and poly(methylphenylsilylene) blocks. We provide a brief précis of the theoretical background to SQELS, which sets out the parameters accessible and indicates how they may be interpreted. This is followed by the details of the polymer and surface light scattering experiments, the results of which are then discussed.

Theory

Liquid surfaces are continually perturbed by thermal fluctuations, which can be decomposed into a discrete set of Fourier modes, each of a particular wavenumber. The frequency and wavenumber of these Fourier modes, known as capillary waves, are linked by the dispersion equation. For pure liquid surfaces, the physical parameters in the dispersion equation are the viscosity, the density, and the surface tension, and the first-order approximations to the capillary wave frequency, ω_0, and damping, Γ (that together form the complex frequency of the capillary wave, see eq 5), are given by

$$\omega_0 = \left(\frac{\gamma_0 q^3}{\rho}\right)^{1/2} \tag{1}$$

$$\Gamma = \frac{2\eta q^2}{\rho} \tag{2}$$

where η, ρ, and γ_0 are the viscosity, density, and surface tension of the liquid and q is the surface wavenumber observed.

Lucassen[44,45] demonstrated that, in the presence of a second species (either as a spread film or as a surface excess), in addition to these transverse capillary modes, a longitudinal dilational mode appears at the surface. This was later identified by Goodrich[46] as one of five possible surface dynamic modes, these modes being (i) transverse shear, (ii) lateral compression (the dilational mode), (iii) lateral shear, (iv) horizontal shear or slip, and (v) vertical compression. Both the transverse and dilational modes have an associated modulus. The transverse modulus is the surface tension (γ), and the longitudinal modulus is the dilational modulus (ϵ). The resulting dispersion equation is given by

$$D(\omega) = [\epsilon q^2 + i\omega(m+q)][\gamma q^2 + i\omega(m+q) - \omega^2\rho/q] + [\omega\eta(q-m)]^2 \tag{3}$$

where q is the capillary wavenumber selected and ρ is the liquid density that also has a viscosity η. The parameter m is defined by

$$m = (q^2 + i\omega\rho/\eta)^{1/2} \tag{4}$$

and ω is the complex frequency of the capillary wave, expressed in terms of the real frequency (ω_0) and the damping, Γ.

$$\omega = \omega_0 + i\Gamma \tag{5}$$

The capillary waves can be viewed as an optical grating at the liquid surface, and although of small amplitude, they scatter light efficiently. Because of energy transfer between the capillary waves and photons, the energy distribution of the scattered light is broader than that of the incident light. The power spectrum of this scattered light is

$$P(\omega) = -(k_B T/\pi\omega)\,\mathrm{Im}\left[\frac{i\omega\eta(q+m) + \epsilon q^2}{D(\omega)}\right] \tag{6}$$

Analysis of the power spectrum (or the correlation function if the temporal rather than frequency evolution is monitored) of the scattered light thus permits, in principle, the evaluation of γ and ϵ. The transverse and dilational surface modes are always coupled, and since they are oscillatory, there is the possibility of resonance between the modes occurring, i.e., both modes having the same frequency. For a spread film both γ and ϵ are dependent upon the surface concentration and the capillary wave frequency. Consequently, resonance would manifest itself as a maximum in frequency and damping at a particular surface concentration. The surface moduli are complex quantities and can be expanded as linear response functions that will incorporate dissipative effects:

$$\gamma = \gamma_0 + i\omega\gamma' \tag{7}$$

$$\epsilon = \epsilon_0 + i\omega\epsilon' \tag{8}$$

where γ_0 and ϵ_0 are the surface tension and dilational modulus at the capillary wave frequency and the associated primed terms are the transverse shear and dilational viscosities. Recently the existence of a transverse shear viscosity has been questioned; Buzza et al.,[33] using a brush model of polymers at liquid interfaces, asserted that γ' is nonexistent. The dispersion equation obtained from this molecularly based theory contains additional parameters. However, it is predicted that the contribution of these parameters depends on the existence of a brushlike surface layer thickness of ca. 1 μm at the wavenumbers accessible to light scattering techniques. Therefore, these additional parameters will be presumed as negligible for the system discussed here. The parameters γ_0, ϵ_0, and ϵ' are retained, and the

incorporation of γ' into the analysis of SQELS data may result in "effective" parameters being obtained because the dispersion equation used is not an accurate representation. A close examination of the wavenumber dependency of the capillary wave frequency and damping is valuable in determining the processes in operation.

Experimental Section

Polymer Synthesis and Characterization. In accordance with the first reaction of Scheme 1, PMPS was synthesized by reaction of dichloromethylphenylsilane with a sodium dispersion in THF at room temperature using the Wurtz-type reductive coupling reaction. After 3 h of reaction the product, α,ω-dichloropoly(methylphenylsilylene) of $\bar{M}_n = 13\,100$ (by size exclusion chromatography using polystyrene standards) and $\bar{M}_w/\bar{M}_n = 3.3$, was precipitated by addition of the liquid phase to dried petroleum ether under strictly anhydrous conditions. A solution of the polymer in THF was then treated with an excess of bromine in order to reduce the degree of polymerization. The molecular weight parameters of what was now predominantly an α,ω-dibromopoly(methylphenylsilylene) were $\bar{M}_n = 5280$ and $\bar{M}_w/\bar{M}_n = 1.72$.

Using Schlenk-line techniques, as depicted in Scheme 2, the above sample of PMPS was reacted with an equimolar amount of a dried, narrow distribution poly(ethylene glycol) in THF at room temperature using pyridine as a dehydrohalogenating agent. The PEO, supplied by Aldrich, was of nominal molecular weight 8000 but characterized by gel permeation chromatography, GPC, to have $\bar{M}_n = 7010$ and $\bar{M}_w/\bar{M}_n = 1.03$. The product was isolated by fractional precipitation using methanol and pentane. GPC and ^{1}H NMR analysis showed it to be a multiblock copolymer of $\bar{M}_n = 26\,700$ and $\bar{M}_w/\bar{M}_n = 1.57$ and an average structure corresponding to $(PMPS-PEO)_2-PMPS$.

Surface Pressure Isotherms. The surface pressure isotherm of the block copolymers at 298 K was obtained by the dropwise addition of a chloroform solution of the copolymer (ca. 0.5−1.0 mg cm^{-3}) to the surface of a freshly aspirated ultrapure water subphase (Elga UHQ II) in a Langmuir trough (model 601A, Nima Ltd). Spread layers occupied an area of some 580 cm^2 and were left for a minimum of 20 min to allow complete solvent evaporation and film relaxation prior to compression. The film was then compressed and the surface pressure continuously recorded using a Wilhelmy plate. Compression rates from 30 to 60 cm^2 min^{-1} were used, but there was no influence of this rate on the isotherms obtained.

Surface Quasi-Elastic Light Scattering. The small energy transfers involved in SQELS are such that heterodyne optical methods are mandatory. A detailed description of the optical system has been published earlier;[47] specific details were the use of a solid-state continuous wave laser of 100 mW output at a wavelength of 532 nm as the light source. Scattered light from the liquid surface was mixed with a weak reference beam and was incident on a photomultiplier tube, the output from which was passed to a Brookhaven BI9000 correlator. The SQELS data were thus collected in the temporal domain rather than the frequency domain. The correlation functions were analyzed by two methods. First, the frequency (ω_0) and damping (Γ) of the capillary waves were obtained by fitting of a damped cosine equation which included a phase shift term to model the non-Lorentzian nature of the power spectrum of the scattered light. This provides objective values of the capillary wave frequency and damping and does not rely on any theoretical description. Second, the surface light scattering data were analyzed by the direct spectral fitting method pioneered by Earnshaw et al. some years ago and described in detail elsewhere.[48−50] This method uses the dispersion equation to generate a theoretical form of the correlation function, which is then fitted to the data by adjusting the surface moduli, γ and ϵ. Consequently, the values obtained depend on the exact form of the dispersion equation used. In view of the debate over the existence of γ', we have analyzed the data in two ways: first the transverse shear viscosity has been fixed at zero, second it was allowed to be a fitting variable along with the other surface viscoelastic parameters.

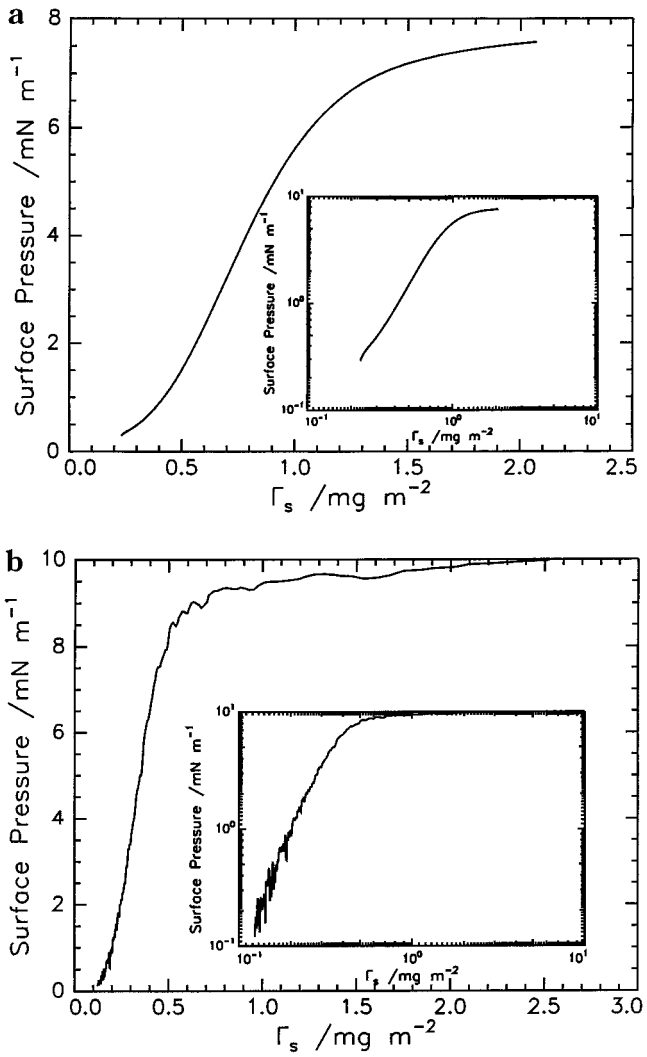

Figure 1. (a) Surface pressure isotherm for the spread copolymer at 293 K; inset is a double-logarithmic plot of the data. (b) Surface pressure isotherm for poly(ethylene oxide).

Results

Surface Pressure Isotherms. A typical surface pressure isotherm is shown in Figure 1a, and for comparison the surface pressure isotherm for PEO homopolymer is given in Figure 1b. Clearly there are common features which suggests that it is the PEO component that determines the surface pressure behavior. In each case the surface pressure increases smoothly to a plateau, this increase being slower for the copolymer due to the "dilution" of the PEO on the surface by the silylene blocks in the copolymer and probably the polydispersity of the copolymer. However, there are differences that deserve comment. The plateau surface pressure of ca. 7.5 mN m^{-1} obtained at $\Gamma_s \sim 1.5$ mg m^{-2} for the copolymer is low in comparison; both linear and cyclic PEO homopolymers which have plateau surface pressures of ∼9.5 mN m^{-1} were obtained at $\Gamma_s \sim 0.5$ mg m^{-2}.[31,51] The inset in Figure 1a is a double-logarithmic plot of the surface pressure data, and between surface concentrations of 0.5 and 1.0 mg m^{-2} there is a linear region. Linear least-squares fitting to this region provides the following scaling relation:

$$\pi \sim \Gamma_s^{2.3}$$

The scaling exponent for the surface pressure of PEO

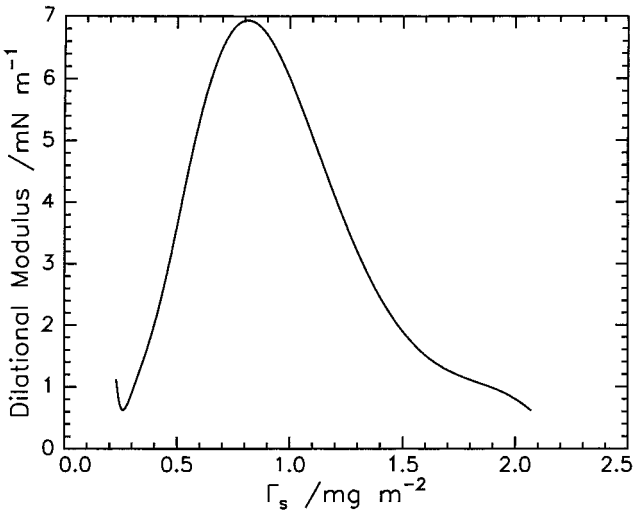

Figure 2. Dilational modulus calculated from the surface pressure isotherm of Figure 1a.

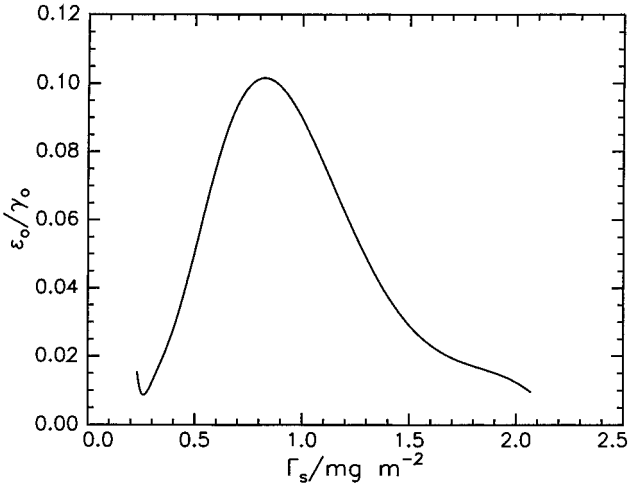

Figure 3. Ratio of dilational modulus to surface tension calculated from surface pressure isotherm.

homopolymer is ~ 3.5. For homopolymers this scaling exponent can be related to the nature of the thermodynamic interaction between polymer and subphase.[52,53]

The surface pressure isotherm data were fitted by an empirical polynomial and the dilational modulus (Gibbs elasticity) evaluated using the relation

$$\epsilon_0 = \Gamma_s \frac{d\pi}{d\Gamma_s} \tag{9}$$

Figure 2 shows the variation of the static dilational modulus with surface concentration of the block copolymer; a maximum value is obtained at 0.8 mg m^{-2}, the inflection point of the surface pressure isotherm of Figure 1a. The magnitude of the dilational modulus is small, and for surface concentrations greater than ~1.0 mg m^{-2} it decreases rapidly to values approaching zero. The possibility of resonance between transverse and dilational modes was mentioned earlier when the principles of surface light scattering were set out. To ascertain whether the possibility would occur in the surface concentration range explored for the block copolymer, the ratio of the static values of ϵ_0 and γ_0 is plotted in Figure 3; this plot suggests that resonance should not be observed in the light scattering data because the resonance condition of $\epsilon_0/\gamma_0 = 0.16$ is not approached over the range of surface concentrations explored.

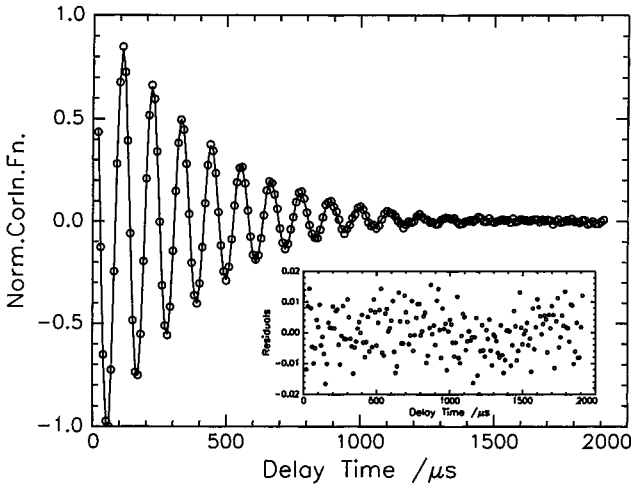

Figure 4. Experimental correlation function and a fit to the data (solid line) for $q = 353$ cm^{-1} and $\Gamma_s = 0.65$ mg m^{-2}. The inset shows the residuals from the fitting process.

Surface Quasi-Elastic Light Scattering. Figure 4 shows a typical normalized correlation function for the copolymer with a surface concentration of 0.65 mg m^{-2} obtained at $q = 352$ cm^{-1}; the inset shows the residuals with the line through the data which is the fit from the spectral fitting method outlined above. In general, the deviation of the fitted line from the data was ±2% over the whole range of delay times used. A series of experiments were undertaken to assess the coherence of the spread layer, i.e., ascertain whether the spread film was "patchy" at any surface concentrations. For this purpose correlation functions were repeatedly collected over a period of 2 h for four values of Γ_s and then analyzed for the frequency and damping of the capillary waves. The frequencies obtained are displayed as histograms in Figure 5. At the lowest surface concentration (0.14 mg m^{-2}) it is clear that the data fall into two groups: one group has a frequency slightly different from that of the clean water surface, and the second group has a distinctly higher frequency although this has a wide distribution. Increasing the surface concentration to 0.25 mg m^{-2} results in the frequency data being somewhat broadly distributed about a mean value. For higher surface concentrations, the distribution of capillary wave frequency is narrow. Evidently at the lowest surface concentration, the coverage of the water surface by the copolymer is incomplete, and there are "islands" of copolymer on the surface. The breadth of the frequency distribution for $\Gamma_s = 0.25$ mg m^{-2} suggests that the surface concentration of the spread film may not be identical over the whole area. For higher concentrations, this inequality of concentration appears to have disappeared, and we presume the film is coherent over the whole area.

Initial SQELS experiments used a rather coarse division of surface concentration to ascertain regions of interest. These data were combined with data obtained using a finer variation in Γ_s. The value of q used was ca. 353 cm^{-1} for both sets of experiments, but inevitably there are small differences between them because of the impossibility of obtaining exactly the same alignment between separate experiments. (The most sensitive factor is the height of the liquid surface; small variations

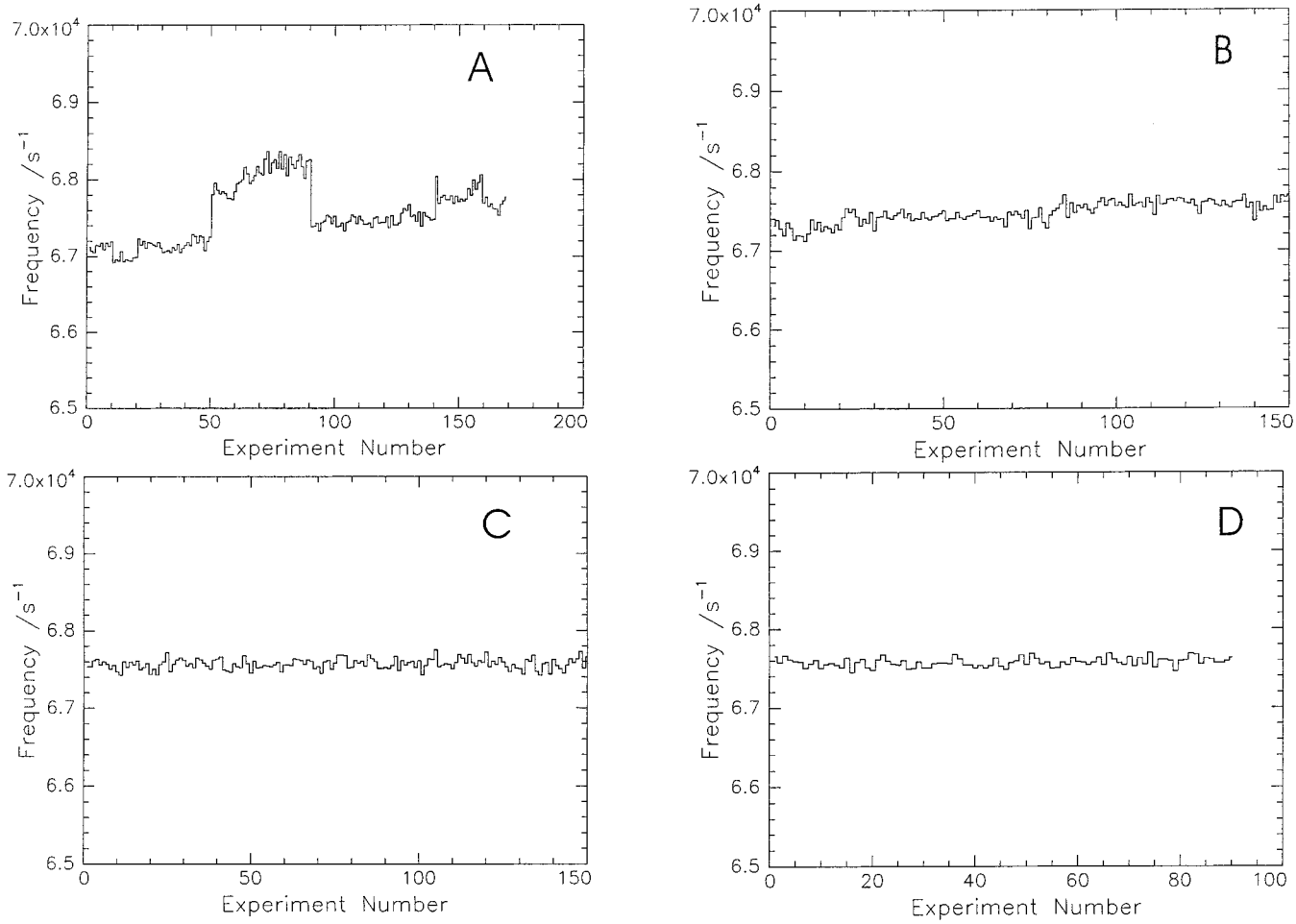

Figure 5. Distribution of capillary wave frequencies at selected average surface concentrations of (A) 0.14, (B) 0.25, (C) 0.38, and (D) 0.50 mg m^{-2} and $q = 397$ cm^{-1}.

in this can produce significant changes in q.) Variations in the two sets of data are illustrative of the sensitivity of the technique and its ability to respond to very small changes in any parameter, either instrumental or associated with the sample. Figure 6 shows all the frequency and damping data over a surface concentration range of 0.25−2.0 mg m^{-2}. Each of the points is the average value calculated from a minimum of 10 individual correlation functions each separately analyzed; the error bars for these data are within the size of the symbols in Figure 6. The capillary wave frequency increases smoothly with increasing Γ_s, displaying a maximum at 0.65 mg m^{-2}, whereafter it falls rapidly but seems to approach an asymptotic value in the surface concentration range 1.0−1.8 mg m^{-2}. This region corresponds to the broad "shoulder" in the surface pressure isotherm as the asymptotic surface pressure is approached. The capillary wave damping rises sharply to a maximum at $\Gamma_s = 0.8$ mg m^{-2} where the damping is approximately twice that of the clean air/water interface. There appears to be small oscillations in Γ (just outside the experimental error) superimposed on a slow decrease in the magnitude of the damping as the surface concentration increases to 1.75 mg m^{-2}. The damping falls steeply at higher surface concentrations, but there are only two data points in this region. This increase and observation of a maximum in the damping are clear symptoms of resonance and contradict the expectations based on Figure 3; i.e., there would be no resonance between capillary and dilational modes. To determine whether this is due to a classical resonance, we must evaluate the surface viscoelastic parameters.

To obtain these, the data were analyzed using the direct spectral fitting method, for which the following constraints were applied: γ_0 and ϵ_0 values returned had to be positive, γ' was fixed at zero, in agreement with a recent molecularly based theory of surface quasi-elastic light scattering,[33] but ϵ' was allowed to have either positive or negative values returned by the fitting process. This direct fitting is sensitive to the starting values used because the large parameter space explored has many local minima in the criterion of goodness of fit. Fits were repeated exploring a wide range of starting values for each surface concentration; a majority settled on the same set of final values. From this analysis, the final set of values for γ_0, ϵ_0, and ϵ' as a function of Γ_s are shown in Figure 7 for $q \sim 353$ cm^{-1} and at a temperature of 293.8 K. In Figure 7a the surface tension obtained from the surface pressure isotherm is also plotted; the light scattering values show a similar dependence on concentration as the static values but in general are of slightly larger magnitude. Evidently there is a relaxation process in the spread copolymer film when it is perturbed by a capillary oscillation. The dilational modulus obtained by SQELS has no correspondence with that of Figure 2; a maximum value is not obtained, and moreover the plateau value of ca. 15 mN m^{-1} is considerably larger than the static values in this region of concentration, which again indicates a considerable relaxation process in the dilational mode

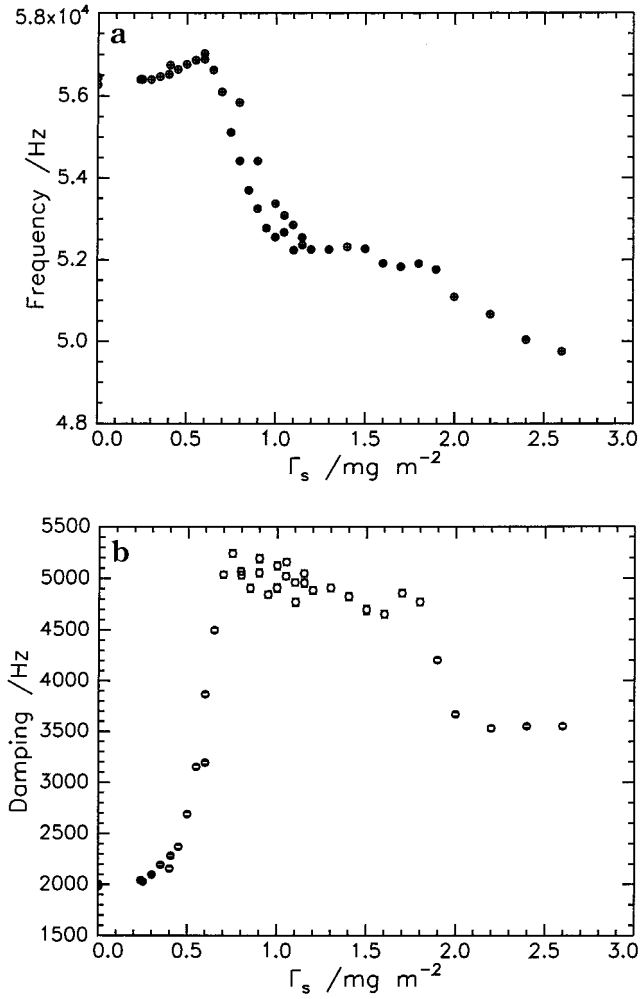

Figure 6. Capillary wave (a) frequency and (b) damping as a function of the spread-layer concentration at a temperature of 294 K. The error bars are smaller than the symbols and were obtained from values of frequency and damping for 10 separate correlation functions.

in response to perturbation. The dilational viscosity is negative at low surface concentrations, and then at Γ_s ca. 0.6−0.7 mg m^{-2} it steadily increases to an approximately constant value of ca. 5×10^{-4} mN m s^{-1}. This is quite different from the behavior of PEO homopolymer,[31] for which ϵ' is initially positive and decreases with increasing Γ_s, values becoming negative for $\Gamma_s \geq 0.6$ mg m^{-2} where the polymer penetrated the subphase to a finite depth. The values of ϵ_0/γ_0 obtained from the light scattering data are plotted in Figure 8 as a function of Γ_s, and a value of 0.16, the condition for resonance to be observed, is obtained at ca. 0.8 mg m^{-2}. This was sufficiently close to the surface concentration where the maximum damping was observed for us to associate this maximum with a classical resonance between the dilational and capillary modes.

For a fixed surface concentration of 0.8 mg m^{-2}, the capillary wave frequency and damping were investigated as a function of q, and the values are shown in Figure 9 together with the theoretically calculated values for the clean water surface from the dispersion equation. In the double-logarithmic plot of Figure 9, the frequency data are essentially linear whereas the capillary wave damping exhibits a definite change in q dependence for values greater than ∼700−800 cm^{-1}. Surface viscoelastic parameters obtained at each q are

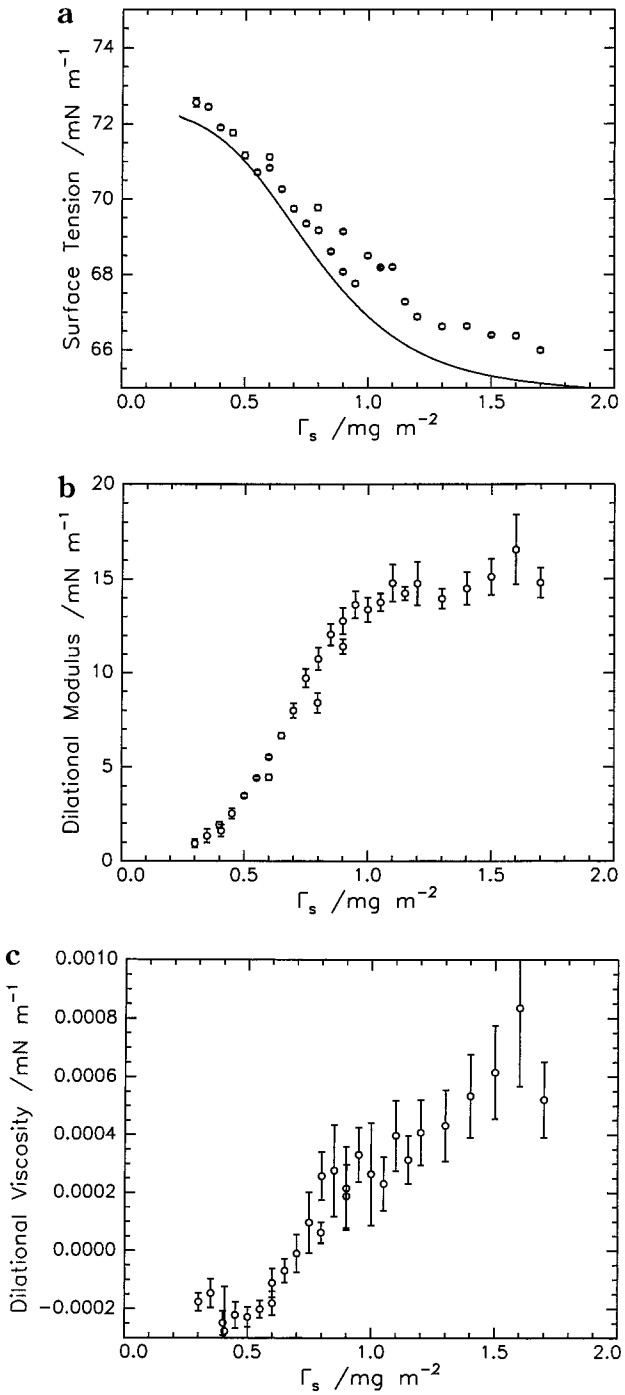

Figure 7. Surface viscoelastic parameters from surface light scattering as a function of surface concentration of copolymer: (a) surface tension, (b) dilational modulus, and (c) dilational viscosity. The line in (a) is the surface tension from the surface pressure data, i.e., the $\omega_o = 0$ value, and the error bars were obtained by fitting to 10 separate correlation functions.

plotted as a function of surface wave frequency in Figure 10. Both moduli (surface tension and dilational modulus Figure 10a,b) exhibit the same broad dependence in frequency. There is an initial decrease in both moduli until a frequency of ca. 300 kHz ($\equiv q \sim 1000$ cm^{-1}); thereafter, the moduli increase with increasing surface wave frequency. Similar behavior is not observed in the dilational viscosity. In general, the dilational viscosity starts with negative values at low frequencies and just becomes positive at a capillary wave frequency of ca. 400 kHz.

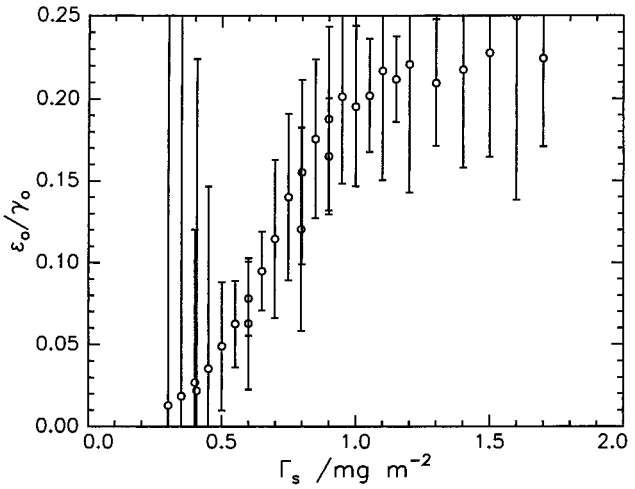

Figure 8. Ratio ϵ_0/γ_0 as a function of Γ_s from light scattering data at $q = 353$ cm^{-1}.

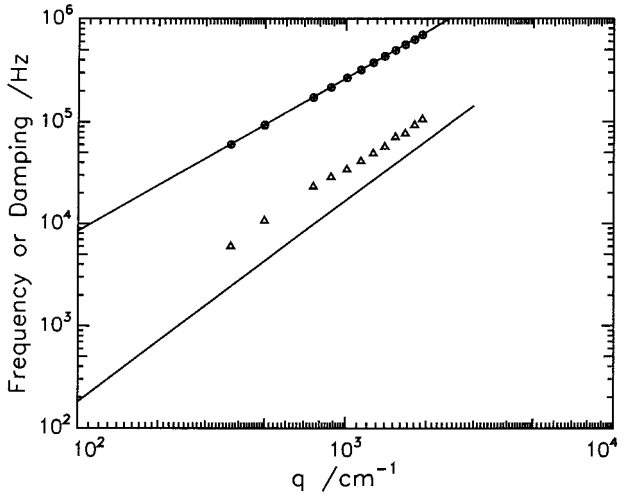

Figure 9. Capillary wavenumber (q) dependence of the frequency and damping for a spread copolymer film with $\Gamma_s = 0.80$ mg m^{-2}. Lines are calculated from solving the dispersion equation for a clean water surface.

Discussion

For spread homopolymer films the exponent, y, in the surface pressure−surface concentration relation is related to the excluded-volume factor n by the equation[52]

$$y = 2\nu/(2\nu - 1)$$

Thermodynamically favorable interactions between spread polymer and subphase are indicated for a ν value of 0.75, a value observed for spread films of poly(ethylene oxide). Although this treatment is not strictly applicable to spread films of block copolymers, the value of y observed here suggests that ν approaches a value of 0.9 because the scaling relation for the surface pressure observed over the initial linear region was $\pi \sim \Gamma^{2.29}$. This high value may be symptomatic of the stiff rodlike nature of the polysilylene blocks flanking the poly(ethylene oxide) blocks. This structure also means that there are no "tails" of poly(ethylene oxide) in the aqueous subphase, and any penetration of the subphase must be confined to loops. Consequently, we do not anticipate exploration to great depths of the subphase by the PEO. In this respect, the situation is somewhat akin to an earlier investigation[51] of cyclic poly(ethylene oxide) where loop structures were intrinsic to the molecular architecture. This system exhibited negative dilational viscosities over the whole spread film surface concentration range examined.

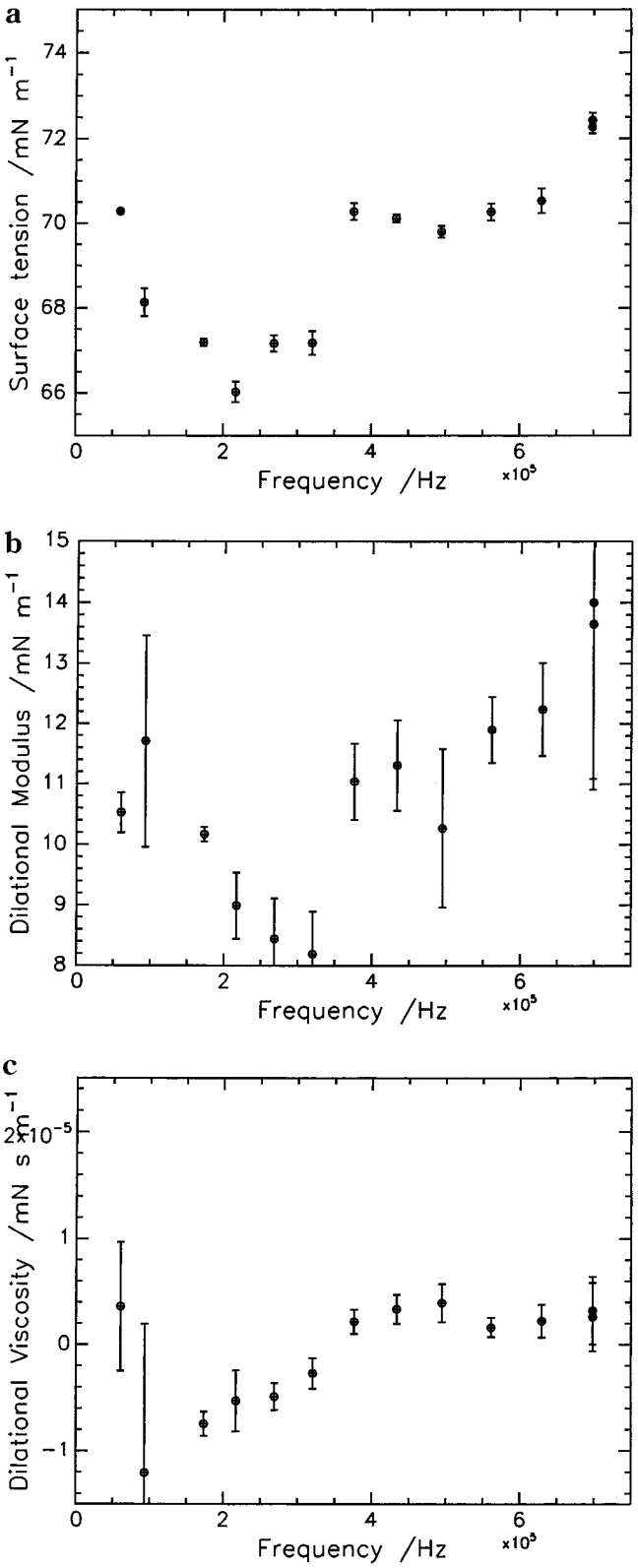

Figure 10. Dependence of surface viscoelastic parameters on capillary wave frequency for $\Gamma_c = 0.8$ mg m^{-2} at 294 K. (a) γ_0, (b) ϵ_0, (c) ϵ'. Error bars are estimated from fits to 10 individual correlation functions.

A molecular description of surface viscoelastic parameters has been provided by Buzza et al.[33] for the case where the polymer film can be described as a brushlike

layer. The air−water interface is viewed as having a grafting density, σ, of molecules with a degree of polymerization of N and statistical step length b; the various surface viscoelastic parameters are then given by

$$\pi \approx \sigma^{11/6} b^{5/3} N k_B T \tag{10}$$

$$\epsilon \approx \sigma^{11/6} b^{5/3} N k_B T \tag{11}$$

$$\epsilon' \approx \sigma^2 \eta b^5 N^3 \tag{12}$$

where η is the viscosity of the fluid phase that surrounds the brush layer. These equations indicate that there are no factors that could be responsible for making ϵ' negative. Such negative values have been attributed to the failure of the dispersion equation to account for other factors, notably a coupling coefficient and the bending modulus of the surface film. The bending modulus is generally disregarded because values are very small, and the factor only becomes significant when the surface tension approaches zero.[43] The coupling coefficient connects surface perturbations to changes in concentration of the brush layer at finite depths below the surface, and it has an associated viscosity term. However, this term only becomes important for the range of q accessible to visible light when the spread layer thickness in the subphase approaches 1 μm. Such layer thicknesses have never been observed; moreover, the formation of a brushlike layer from solvated polyethylene bocks in these multiblock copolymers is precluded by their architecture. For solutions where surface excess layers are formed, negative dilational viscosities arise naturally when the surface layer is not in equilibrium with the bulk concentration at greater depths.[54] Clearly, this cannot be the case here because the copolymer is insoluble in water. We have to resort to accepting that the dispersion equation may be inadequate for this situation, and the dilational viscosity values obtained are *effective* values. Phenomenologically, negative values of ϵ' correspond to a reduction of the damping of the dilational waves compared to that when $\epsilon' = 0$.

Evidently there are relaxation processes taking place in the spread film following perturbation by surface waves, since the surface tension and the dilational modulus obtained by SQELS at $q = 353$ cm^{-1} are larger than those obtained at zero frequency (i.e., from the surface pressure data). This is particularly true for the dilational modulus values. The relaxation mechanism can be obtained by comparing the frequency dependence of the various surface moduli with that predicted by relatively simple models. However, because we are unable to observe the dilational wave frequency directly, examination of the dilational modes in this way means that we have to be at the resonance condition because only at this point is the dilational wave frequency equal to the observable capillary wave frequency. Additionally, because of the coupling of the two modes at the resonance condition, the capillary waves have maximum sensitivity to the dilational wave properties. Unfortunately, the data in Figure 10 do not conform to any of the commonly used models for viscoelasticity,[55] e.g., a Maxwell or Voigt fluid. In fact, remarkable changes in behavior of the surface parameters with frequency are observed.

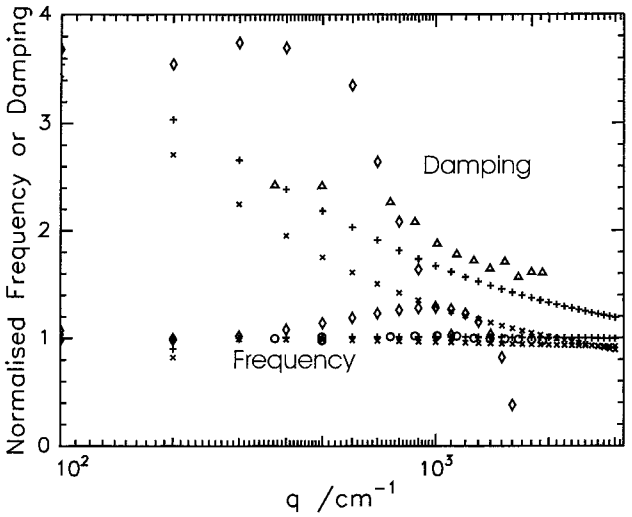

Figure 11. Normalized capillary wave damping and frequency as a function of wavenumber. Experimental data: damping, △; frequency, ○. Other data calculated for the following conditions: $\gamma_0 = 68$ mN m^{-1}, $\epsilon_0 = 10$ mN m^{-1}, and (+) $\epsilon' = 0$, (×) $\epsilon' = 5 \times 10^{-5}$ mN s m^{-1}, and (◊) $\epsilon' = -5 \times 10^{-5}$ mN s m^{-1}.

Plotting normalized frequency and damping, i.e., capillary wave frequency and damping divided by the values calculated from the first-order eqs 1 and 2, as a function of q (Figure 11) gives a clue to what is happening. These experimental values are compared with the predictions obtained by solving the dispersion equation for the situation where $\gamma_0 = 68$ mN m^{-1} and $\epsilon_0 = 10$ mN m^{-1} for three different values of ϵ'. The value of ϵ' has little influence on the capillary wave frequency, and as long as $\epsilon' \geq 0$, then the capillary wave damping decreases as q increases. However, for $\epsilon' = -5 \times 10^{-5}$ mN s m^{-1}, the calculated normalized damping has a plateau value for q values less than ∼500 cm^{-1}, and the q dependence of the capillary wave damping has a form remarkably similar to that observed. A double-logarithmic plot (Figure 12) of these various predicted surface wave behaviors is very revealing. For $\epsilon' = 0$, linear dependencies on q of both capillary wave and dilational wave frequency and damping are predicted over all q values. Moreover, the exponent in the q dependence of the various frequencies and dampings conforms with the first-order predictions. When ϵ' is positive and larger than zero, the real frequency of the dilational mode begins to decrease at high q, as does the dilational damping albeit at a somewhat slower rate. For negative values of ϵ' quite different behavior is observed. Now the capillary wave frequency turns over and vanishes at high q. At the same time the dilational wave frequency acquires a stronger dependency on q and takes on the characteristics of capillary waves. Likewise, the capillary wave damping disappears, and the dilational wave damping takes on the features of capillary waves. This behavior is characteristic of mode mixing, and this occurs when the damping of the two modes is identical. In the absence of a finite transverse shear viscosity, the only factor in the dispersion equation that can reduce the dilational wave damping to bring it into coincidence with that of the capillary wave is by having a negative dilational viscosity. When the damping of the two modes coincides, the character of the surface mode frequencies changes—the mode that was initially capillary-like in nature taking on characteristics of the dilational mode and vice versa. This behavior is il-

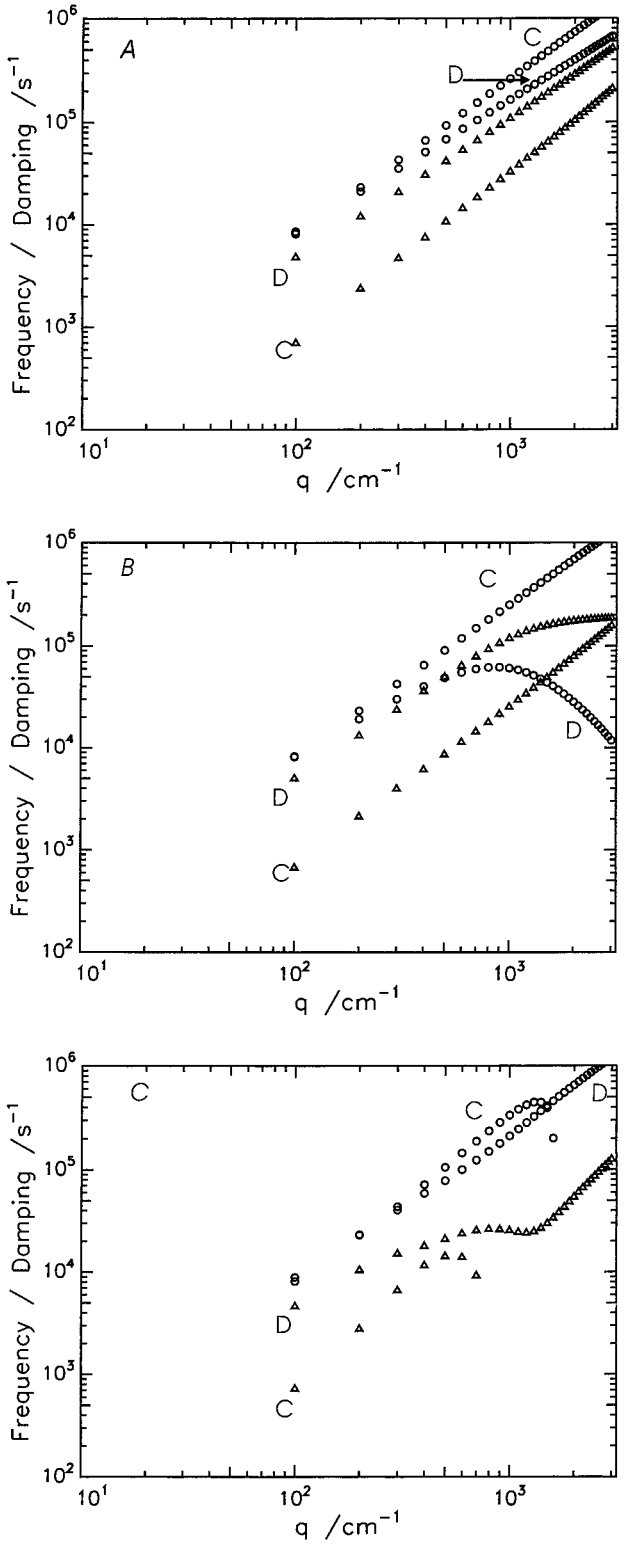

Figure 12. Double-logarithmic plots of frequency (○) and damping (Δ) for dilational and capillary waves as a function of q for (A) $\gamma_0 = 68$ mN m^{-1}, $\epsilon_0 = 10$ mN m^{-1}, $\epsilon' = 0$ mN m s^{-1}; (B) $\gamma_0 = 68$ mN m^{-1}, $\epsilon_0 = 10$ mN m^{-1}, $\epsilon' = 5 \times 10^{-5}$ mN m s^{-1}; (C) $\gamma_0 = 68$ mN m^{-1}, $\epsilon_0 = 10$ mN m^{-1}, $\epsilon' = -5 \times 10^{-5}$ mN m s^{-1}. C = capillary modes, D = dilatational modes.

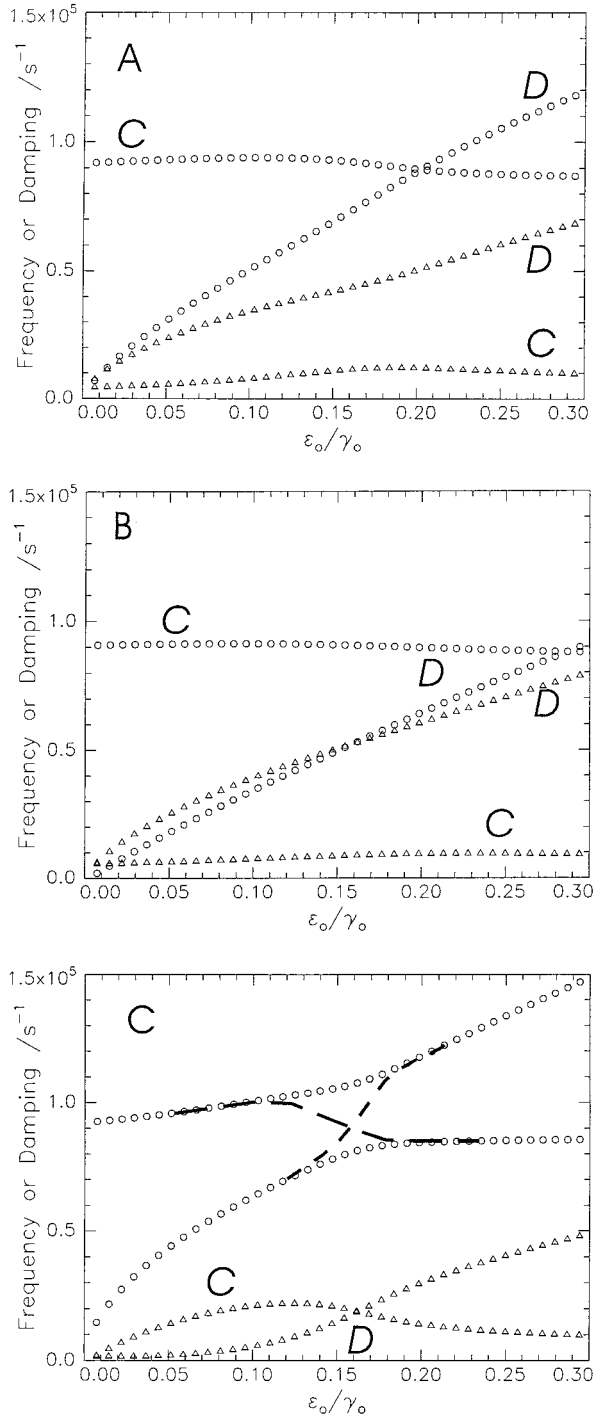

Figure 13. Frequency and damping of capillary and dilational modes calculated as a function of ϵ_0/γ_0 for $\gamma_0 = 68$ mN m^{-1}, $q = 500$ cm^{-1}, and (A) $\epsilon' = 0$, (B) $\epsilon' = 5 \times 10^{-5}$, and (C) $\epsilon' = -5 \times 10^{-5}$ mN s m^{-1}. Italic *C* and *D* indicate capillary and dilational modes, respectively; ○ = frequencies, Δ = damping. The dashed lines in (c) are indicative of the crossover in behavior of capillary and dilatational waves.

lustrated in Figure 13 where frequency and damping have been calculated as a function of ϵ_0/γ_0. Mode mixing is observed when the damping of the capillary and dilational modes becomes equal, and this at the resonance point. Splitting between the frequencies of the two modes at the mode mixing point is seen in the theoretical plots, and this becomes increasingly evident as ϵ' becomes more negative. A more explicit demonstration of the differences in behavior is evident if the surface wave dispersion is plotted in the complex plane as in Figure 14. For $\epsilon' = 0$, the capillary mode comes down more or less vertically at the normalized frequency of 1 with the dilational mode sweeping downward from right to left. Increasing ϵ' has no significant effect on the nature of the capillary mode dispersion; the dila-

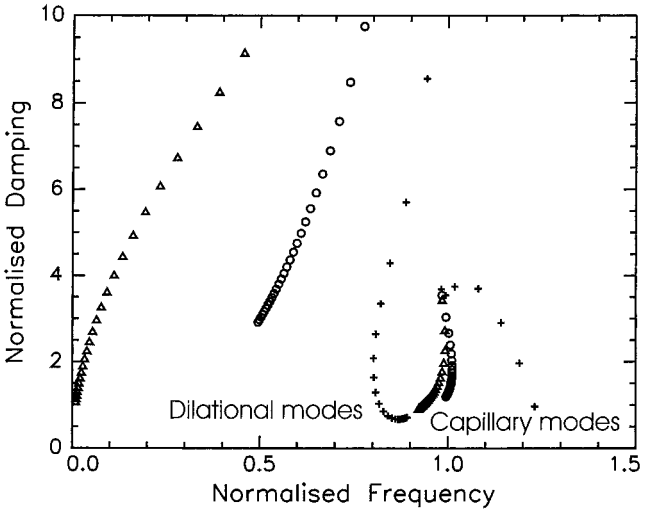

Figure 14. Data of Figure 11 plotted in the complex plane and illustrative of the very different behavior anticipated in experimental data dependent on the values of ϵ': (○) $\epsilon' = 0$; (△) $\epsilon' = 5 \times 10^{-5}$ mN s m^{-1}, (+) $\epsilon' = -5 \times 10^{-5}$ mN s m^{-1}.

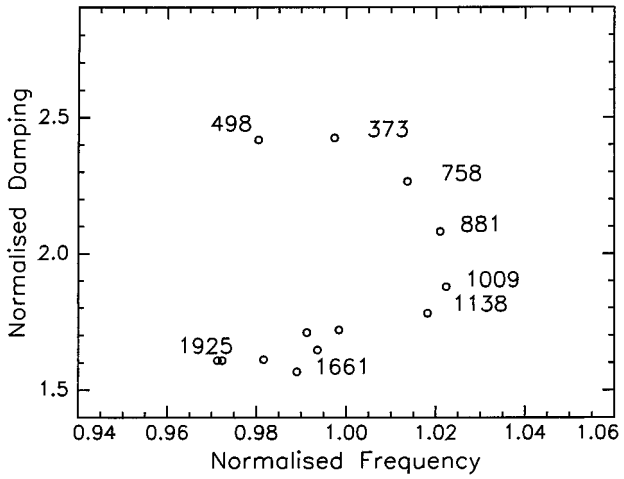

Figure 15. Normalized damping and frequency of the silylene−poly(ethylene oxide) block copolymer at a surface concentration of 0.8 mg m^{-2} plotted in the complex plane. The numbers are the q values associated with the data points.

tional mode being more heavily damped at lower frequencies shifts markedly to the left. A negative value for ϵ' causes remarkable changes; first the capillary mode curves upward and to the right before decreasing rapidly and eventually disappearing. The dilational mode in this situation curves down and bends right and up as it approaches the abscissa. Thus, in the presence of mode mixing caused by negative dilational viscosities, we expect the normalized damping to curve upward and to the right as q increases before decreasing along a curved path. At some normalized frequency (q value) the normalized damping should abruptly jump left (but with no significant change in magnitude) as the capillary mode disappears, and the dilational mode dominates the surface modes. Figure 15 shows our data obtained for a spread copolymer film concentration of 0.8 mg m^{-2} (the resonance surface concentration) plotted in the complex plane, and all the features set out above for mode mixing are exhibited. We note that these data are obtained from the directly observable experimental parameters: the frequency and damping of the surface waves. They are *not* dependent on any model for the dispersion of the capillary waves; the only use of a model comes in attempting to ascertain the aspects of the dispersion relation responsible for the observations.

What remains elusive is the molecular basis for the capillary wave behavior. Although the use of effective quantities is acceptable in some areas of physical science (e.g., relativistic aspects), the concept of a negative viscosity is difficult. Although the original definition of surface viscosity by Goodrich does not preclude negative values, no descriptions of the source are forthcoming. We have already noted cases where negative dilational viscosities are physically realistic, but these do not apply here. The most reasonable explanation for negative dilational viscosities is that the dispersion equation is incomplete; i.e., other dynamic modes may be contributing to the observed dispersion that are not explicitly included in the equation. We have referred to, and dismissed as irrelevant here, bending modes and a coupling factor. However, Fan[56] has noted that splay modes may contribute to surface wave dispersion. Given the rigid-rod-like nature of the silylene blocks and the formation of islands noted earlier, then splay modes within these silylene islands may well exist. These modes are sources of additional in plane damping, and this would appear as a net reduction of the dilational mode damping, i.e., a negative dilational viscosity. As the surface concentration increases, the packing of silylene islands increases and splaying of the rodlike blocks becomes more difficult and the contribution decreases. To compensate for the disappearance of this damping mode, the dilational viscosity increases and becomes positive.

One last factor that has not been considered is the possibility of the silylene blocks lifting off the surface into the air phase. This is considered to be extremely remote because of the stiffness of the silylene blocks; moreover, even if such occurrences did happen, their removal from the surface means that they now have no direct influence on the capillary wave dynamics. Such "lift off" would however alter the surface pressure isotherm, but as already remarked, there is nothing unusual about the isotherm.

Conclusions

Multiblock copolymers of poly(methylphenylsilylene) and poly(ethylene oxide) spread at the air−water interface form stable monolayers. The surface pressure−surface concentration scaling in the preplateau region suggests the existence of rigid-rod structures in the spread film. Surface light scattering data show that at low surface concentration the coverage by the block copolymer is "patchy", suggesting aggregation of silylene blocks into randomly distributed islands on the water surface. Capillary wave frequency and damping obtained by SQELS exhibit maxima in their surface concentration dependence, and this is commensurate with a resonance between capillary and dilational waves in the surface film. At the resonance condition, the surface viscoelastic parameters as well as the capillary wave frequency and damping have been obtained over a range of surface wavenumber q. The frequency dependences of the surface moduli were not interpretable by common models of viscoelastic relaxation because of distinct changes in behavior as a function of frequency. Analysis of the frequency and damping of the surface waves leads us to conclude that mode mixing between the two surface waves takes place at the resonance condition. The source of this behavior, as epitomized by

a negative dilational viscosity, is not determinable, but the rigid nature of the silylene blocks may be responsible for a surface splay mode and a source of additional damping that is not properly incorporated into the dispersion equation.

Acknowledgment. We thank the EPSRC for support of the research program of the IRC in Polymer Science of which this work forms part. We also thank the Japan Chemical Innovation Institute under whose management the copolymer syntheses were carried out as part of the Industrial Science and Technology Frontier Programme supported by the Japanese New Energy and Industrial Technology Development Organisation.

References and Notes

(1) Miller, R. D. *Angew. Chem., Int. Ed. Engl. Adv. Mater.* **1989**, *28*, 1733.
(2) Zeigler, J. M.; Harrah, L. A.; Johnson, A. W. *SPIE Adv. Resist Technol. Process. II* **1985**, *539*.
(3) Miller, R. D. *Polym. News* **1987**, *12*, 326.
(4) Yagci, Y.; Onen, A.; Schnabel, W. *Macromolecules* **1991**, *24*, 462.
(5) Abkowitz, M.; Stolka, M. *Philos. Mag. Lett.* **1988**, *58*, 239.
(6) Dohmura, T.; Oka, K.; Yajima, T.; Miyamoto, M.; Nakayama, Y.; Kawamura, T.; West, R. *Philos. Mag. B* **1995**, *71*, 1069.
(7) Kajzar, F.; Messier, J.; Rossilio, C. *J. Appl. Phys.* **1986**, *60*, 3040.
(8) Yang, L.; Wang, Q. Z.; Ho, P. P.; Dorsinville, R.; Alfano, R. R.; Zou, W. K.; Yang, N. L. *Appl. Phys. Lett.* **1988**, *53*, 1245.
(9) Hasegawa, T.; Iwasa, Y.; Koda, T.; Kishida, H.; Tokura, Y.; Wada, S.; Tahiro, H.; Tachibana, H.; Matsumoto, M.; Miller, R. D. *Synth. Met.* **1995**, *71*, 1679.
(10) Wolff, A. R.; West, R. *Appl. Organomet.* **1987**, *1*, 7.
(11) Yucessan, D.; Hostoygar, H.; Denizligil, S.; Yagci, Y. *Angew. Makromol. Chem.* **1994**, *221*, 207.
(12) Yajima, S.; Hasegawa, Y.; Hayashi, J.; Ijmura, M. *J. Mater. Sci.* **1978**, *13*, 2569.
(13) Mazdyasni, K.; West, R.; David, L. D. *J. Am. Chem. Soc.* **1978**, *61*, 504.
(14) West, R. *J. Organomet. Chem.* **1986**, *300*, 327.
(15) Michl, J.; Miller, R. D. *Chem. Rev.* **1989**, *89*, 1359.
(16) Fossum, E.; Love, J. A.; Matyjaszewski, K. *J. Organomet. Chem.* **1995**, *499*.
(17) Demoustier-Champagne, S.; de Mahieu, A. F.; Devaux, J.; Fayt, R.; Teyssie, P. *J. Polym. Chem.* **1993**, *31*, 2009.
(18) Sakurai, H. *Polym. Prepr.* **1990**, *31*, 230.
(19) Lutsen, L.; Jones, R. G. *Polym. Int.* **1998**, *46*, 3.
(20) Lutsen, L.; Cordina, G. P.-G.; Jones, R. G.; Schue, F. *Eur. Polym. J.* **1998**, *34*, 1829.
(21) Holder, S. J.; Hiorns, R. C.; Sommerdijk, N. A. J. M.; Wiliams, S. J.; Jones, R. G.; Nolte, R. J. M. *J. Chem. Soc., Chem. Commun.* **1998**, 1445.
(22) Sommerdijk, N. A. J. M.; Holder, S. J.; Hiorns, R. C.; Jones, R. G.; Nolte, R. J. M. *Proc. Am. Chem. Soc., Div. Polym. Mater: Sci. Eng.*, in press.
(23) Reynolds, I.; Richards, R. W.; Webster, J. R. P. *Macromolecules* **1995**, *28*, 7845.
(24) Richards, R. W.; Rochford, B. R.; Webster, J. R. P. *Faraday Discuss.* **1994**, *98*, 263.
(25) Henderson, J. A.; Richards, R. W.; Penfold, J.; Thomas, R. K. *Acta Polym.* **1993**, *44*, 184.
(26) Henderson, J. A.; Richards, R. W.; Penfold, J.; Thomas, R. K. *Macromolecules* **1993**, *26*, 65.
(27) Henderson, J. A.; Richards, R. W.; Penfold, J.; Thomas, R. K.; Lu, J. R. *Macromolecules* **1993**, *26*, 4591.
(28) Henderson, J. A.; Richards, R. W.; Penfold, J.; Shackleton, C.; Thomas, R. K. *Polymer* **1991**, *32*, 3284.
(29) Peace, S. K.; Richards, R. W.; Williams, N. *Langmuir* **1998**, *14*, 667.
(30) Richards, R. W.; Rochford, B. R.; Taylor, M. R. *Macromolecules* **1996**, *29*, 1980.
(31) Richards, R. W.; Taylor, M. R. *J. Chem. Soc., Faraday Trans.* **1996**, *92*, 601.
(32) Richards, R. W.; Taylor, M. R. *Macromolecules* **1997**, *30*, 3892.
(33) Buzza, D. M. A.; Jones, J. L.; McLeish, T. C. B.; Richards, R. W. *J. Chem. Phys.* **1998**, *109*, 5008.
(34) Crawford, G. E.; Earnshaw, J. C. *Eur. Biophys. J.* **1984**, *11*, 25.
(35) Earnshaw, J. C. *Thin Solid Films* **1983**, *99*, 189.
(36) Earnshaw, J. C.; McGivern, R. C. *J. Phys. D: Appl. Phys.* **1987**, *20*, 82.
(37) Earnshaw, J. C.; McCoo, E. *Langmuir* **1995**, *11*, 1087.
(38) Earnshaw, J. C. *Biochem. Soc. Trans.* **1991**, *19*, 499.
(39) Earnshaw, J. C.; Nugent, C. P.; Lunkenheimer, K. *Langmuir* **1997**, *13*, 1368.
(40) Sakai, K.; Choi, P. K.; Tanaka, H.; Takagi, K. *Rev. Sci. Instrum.* **1991**, *62*, 1192.
(41) Sharpe, D.; Eastoe, J. *Langmuir* **1995**, *11*, 4636.
(42) Sharpe, D.; Eastoe, J. *Langmuir* **1996**, *12*, 2303.
(43) Langevin, D. *Light Scattering by Liquid Surfaces and Complementary Techniques*; Marcel Decker: New York, 1992; Vol. 41.
(44) Lucassen, J. *Trans. Faraday Soc.* **1968**, *64*, 2221.
(45) Lucassen-Reynders, E. H.; Lucassen, J. *Adv. Colloid Interface Sci.* **1969**, *2*, 347.
(46) Goodrich, F. C. *Proc. R. Soc. A* **1981**, *374*, 341.
(47) Richards, R. W.; Rochford, B. R.; Taylor, M. R. *Macromolecules* **1996**, *29*, 1980.
(48) Earnshaw, J. C.; McGivern, R. C. *J. Colloid Interface Sci.* **1988**, *123*, 36.
(49) Earnshaw, J. C.; McGivern, R. C.; McLaughlin, A. C.; Winch, P. J. *Langmuir* **1990**, *6*, 649.
(50) Earnshaw, J. C. *J. Colloid Interface Sci.* **1990**, *138*, 282.
(51) Booth, C.; Richards, R. W.; Taylor, M. R.; Yu, G. E. *J. Phys. Chem. B* **1998**, *102*, 2001.
(52) Kawaguchi, M. *Progr. Polym. Sci.* **1993**, *18*, 341.
(53) Poupinet, D.; Vilanove, R.; Rondelez, F. *Macromolecules* **1989**, *22*, 2491.
(54) Henneberg, M.; Chu, X.-L.; Sanfeld, A.; Velarde, M. G. *J. Colloid Interface Sci.* **1992**, *150*, 7.
(55) Ferry, J. D. *Viscoelastic Properties of Polymers*; Wiley: New York, 1980.
(56) Fan, C. *J. Colloid Interface Sci.* **1973**, *44*, 369.

MA990654W